ELSEVIER

Journal of Alloys and Compounds 446–447 (2007) 276–279

Journal of ALLOYS AND COMPOUNDS

www.elsevier.com/locate/jallcom

Thermal properties of AlH_3-etherate and its desolvation reaction into AlH_3

T. Kato [a,*], Y. Nakamori [a], S. Orimo [a], C. Brown [b], C.M. Jensen [b]

[a] *Institute for Materials Research, Tohoku University, Sendai 980-8577, Japan*
[b] *Department of Chemistry, University of Hawaii, Honolulu, HI 96822, USA*

Received 29 September 2006; received in revised form 14 March 2007; accepted 22 March 2007
Available online 30 March 2007

Abstract

Thermal properties of AlH_3-etherate and its desolvation reaction into AlH_3 were experimentally investigated under heating and isothermal processes. AlH_3-ehterate was desolvated to γ-AlH_3 which immediately transformed into α-AlH_3 in the heating process. The results under the isothermal process provide appropriate conditions to effectively obtain α- and γ-AlH_3 by restraining the occurrence of the dehydriding reaction into metallic Al.

Keywords: Hydrogen absorbing materials; Chemical synthesis; Thermodynamic properties

1. Introduction

Due to a high hydrogen density (10.1 mass%) and a low dehydriding temperature (370–470 K), aluminum trihydride (AlH_3, alane) has recently been regarded as a candidate for hydrogen storage materials [1–3]. AlH_3, with some variations in its crystal structures (α-, α′-, β-, γ-, δ-, ε-, ζ-AlH_3), can be prepared by the desolvation reaction after the chemical reaction between $LiAlH_4$ and $AlCl_3$ in ether [4]. In the chemical reaction, AlH_3-etherate is formed as an intermediate product according to the reaction below [2,5,6]:

$$3LiAlH_4 + AlCl_3 \xrightarrow{ether} 4AlH_3 \cdot n\left[(C_2H_5)_2O\right] + 3LiCl \quad (1)$$

In the desolvation reaction of AlH_3-etherate into AlH_3, the crystal structures of AlH_3 are determined. Although experimental studies on desolvation reactions are believed to be important for optimizing sample preparation conditions, detailed information on these reactions has not been provided so far. In this study, therefore, we investigate the thermal properties of AlH_3-etherate and its desolvation reaction into AlH_3, under both heating and isothermal processes.

* Corresponding author. Tel.: +81 22 215 2093; fax: +81 22 215 2091.
E-mail address: tak-kato@mail.tains.tohoku.ac.jp (T. Kato).

0925-8388/$ – see front matter © 2007 Elsevier B.V. All rights reserved.
doi:10.1016/j.jallcom.2007.03.105

2. Experimental

AlH_3-etherate was prepared based on the method described in the literature [4]. A 1.0 M ether solution of $AlCl_3$ (3.333 g of $AlCl_3$ and 25 mL of ether; powdered $AlCl_3$ with 99.999% purity was purchased from Aldrich) was prepared, and subsequently 100 mL of 1.0 M ether solution of $LiAlH_4$ (solution purchased from Aldrich) was added to the $AlCl_3$ solution. The mixed solution was filtered to remove the LiCl precipitate. The filtrate was evacuated and then heated up to 333 K for 4 h. The final product (AlH_3-etherate) was washed by ether to remove excess $LiAlH_4$, and finally it was evacuated to dryness at 300 K.

The samples were systematically examined by *ex situ* and *in situ* powder X-ray diffraction measurements (XRD, PANalytical X'PERT-Pro with Cu Kα radiation, a semiconductor detector for high-speed measurement within 3 min, and a special chamber with a furnace for *in situ* measurements), Raman spectroscopy (Nicolet Almega-HD with color-CCD, 532-nm laser), thermogravimetry and differential thermal analysis (TG-DTA, Rigaku TG8120, using high-purity helium (>99.99995%) with a flow rate of 150 cm^3/min) and quadrupole mass spectroscopy (QM, Anelva MQA200TS, directly connected with the TG-DTA setups). The samples were always handled in glove boxes filled with purified helium/argon (less than 0.5 ppm oxygen and dew point lower than 200 K).

3. Results and discussion

3.1. Formation of AlH_3-etherate by chemical reaction

The XRD profile and Raman spectrum of our sample are shown in Fig. 1(a) and (b), respectively. As shown in Fig. 1(a), our sample was actually identified as AlH_3-etherate by referring

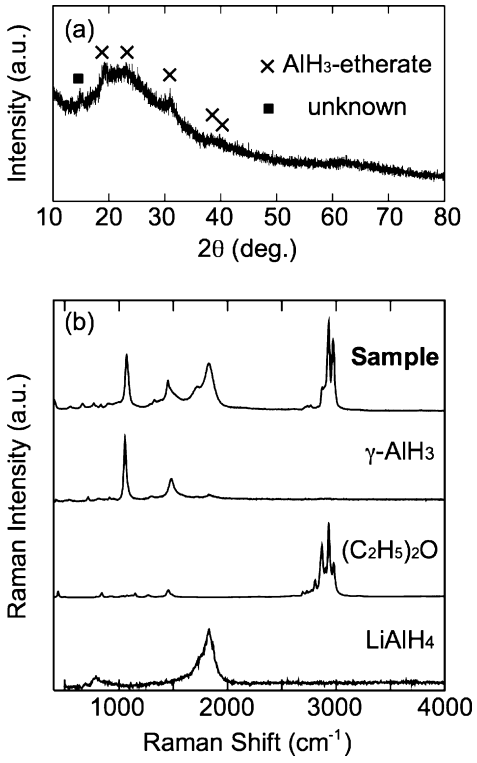

Fig. 1. (a) Powder X-ray diffraction profile and (b) Raman spectrum of our sample (top). Raman spectra of γ-AlH_3, $(C_2H_5)_2O$ and $LiAlH_4$are also shown for references. Raman spectrum of γ-AlH_3 was observed for the first time, and those of $(C_2H_5)_2O$ and $LiAlH_4$ are in good agreement with literatures [7,8].

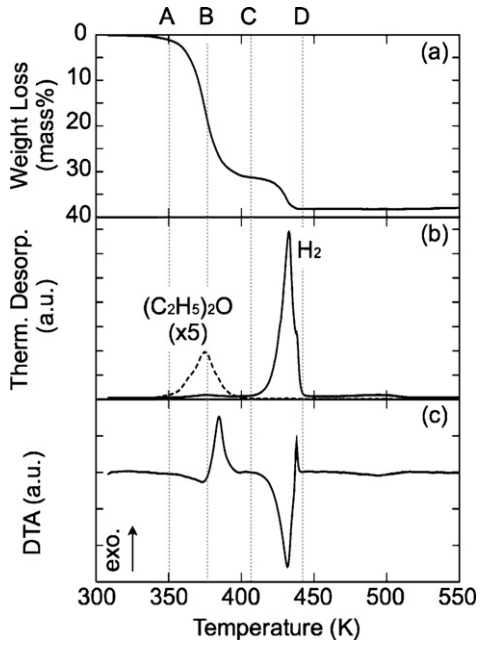

Fig. 2. Results of (a) thermogravimetry, (b) quadrupole mass spectroscopy and (c) differential thermal analysis of AlH_3-etherate, under helium flow with a heating rate of 5 K/min.

to the XRD profile reported in Ref. [4]. As shown in Fig. 1(b), the modes of Raman spectrum were detected for γ-AlH_3, $(C_2H_5)_2O$, and $LiAlH_4$ (residual phase), and these indicated that the Al–H bonding in the AlH_3-etherate prepared in this study was quite similar to that in γ-AlH_3. We consider that this structure determination is valid for the bulk structure because the same spectra shown in Fig. 1(b) were also observed in the samples that were crushed into less than a few micron meters. Although other etherates such as α-AlH_3-etherate were not obtained in our studies, it has not been clarified yet whether γ-AlH_3-etherate is the starting material for the various crystal structures.

3.2. Desolvation and dehydriding reactions under heating process

Fig. 2(a) and (b) shows the results of TG and QM, respectively, after heating. The desolvation reaction of AlH_3-etherate occurred in the temperature range 350–405 K, and subsequently the dehydriding reaction started from approximately 405 K. The weight losses in the desolvation and dehydriding reactions were approximately 31.5 mass% and 6.5 mass%, respectively. These results indicate the molecular formula of the AlH_3-etherate to be $AlH_3{\cdot}0.19(C_2H_5)_2O$.

In the DTA profile shown in Fig. 2(c), the following three peaks, which are derived from the thermal decomposition reactions of AlH_3-etherate, are observed: a broad endothermic peak from 350 K, a subsequent exothermic peak, and a large endothermic peak from 405 K. Two more peaks observed at higher temperatures are due to the residual $LiAlH_4$: a small, sharp exothermic peak at 440 K and a small, broad endothermic peak around 470–520 K. Weight losses were not detected, therefore the amount of residual $LiAlH_4$ was considered to be fairly small.

In order to clarify the origin of the thermal decomposition reactions of AlH_3-etherate, *ex situ* measurements of XRD and Raman spectrum were carried out on the samples that were heated up to 350 K, 373 K, 405 K, and 445 K (shown as temperatures A–D in Fig. 2). As shown in the XRD profiles (Fig. 3(a)), α-AlH_3 and metallic Al were detected at 405 K (temperature C) and 445 K (temperature D), respectively. The Raman spectra corresponding to the XRD profiles (without the metallic Al) are shown in Fig. 3(b). At 373 K (temperature B), only the CH modes of ether around 3000 cm^{-1} were weakened, indicating that AlH_3-etherate was partially desolvated into γ-AlH_3. At 405 K (temperature C), two modes were observed in the range 500–800 cm^{-1} and were attributed to α-AlH_3 [9].

On the basis of the experimental results described above, the steps in the thermal decomposition reactions of AlH_3-etherate are summarized as follows: (I) AlH_3-ehterate is desolvated to form γ-AlH_3 (probably due to the similarity in the Al–H bonding character between them) by an endothermic reaction starting at 350 K, (II) γ-AlH_3 immediately transforms into α-AlH_3 in an exothermic reaction above 373 K, and (III) the dehydriding reaction of α-AlH_3 proceeds along with an endothermic reaction for 405–440 K.

By referring to the enthalpy change for reaction III (9.0 ± 2.3 kJ/mol [4]), the enthalpy change for the entire reaction, as shown in Eq. (2), is calculated to be approximately

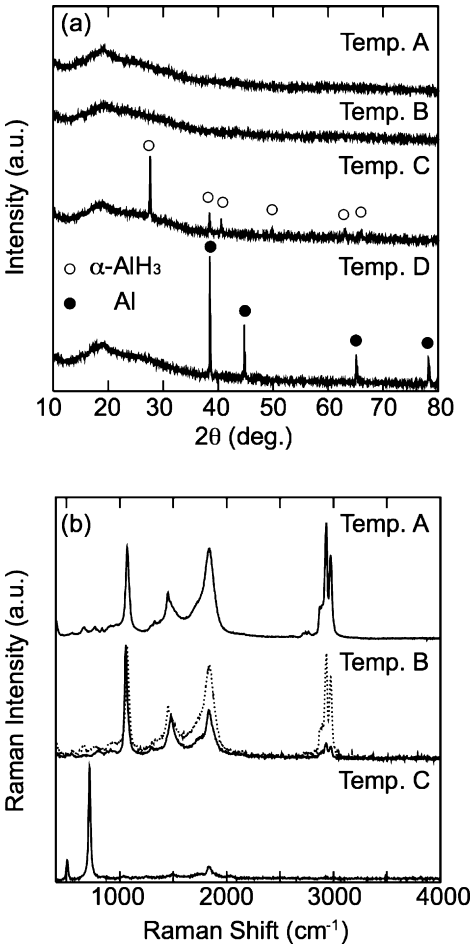

Fig. 3. (a) Powder X-ray diffraction profiles and (b) Raman spectra of the samples that were heated up to the temperatures of 350 K, 373 K, 405 K, 445 K (*ex situ* measurements), corresponding to A–D in Fig. 2, respectively. Dotted line at 373 K (temperature B) is Raman spectrum observed at another point of same sample. Raman spectrum at 405 K (temperature C) is in good agreement with that of α-AlH_3 [9]. No Raman peak was observed at 445 K (temperature D, not shown) because the sample decomposed into the metallic Al.

6 kJ/mol:

$$AlH_3 \cdot 0.19\,[(C_2H_5)_2O]\,(s) \rightarrow Al\,(s) + \tfrac{3}{2}H_2\,(g) + 0.19\,(C_2H_5)_2O\,(g) \quad (2)$$

The standard formation enthalpy of the gas phase of ether is -252.2 ± 0.79 kJ/mol [10]. Therefore, the formation enthalpy

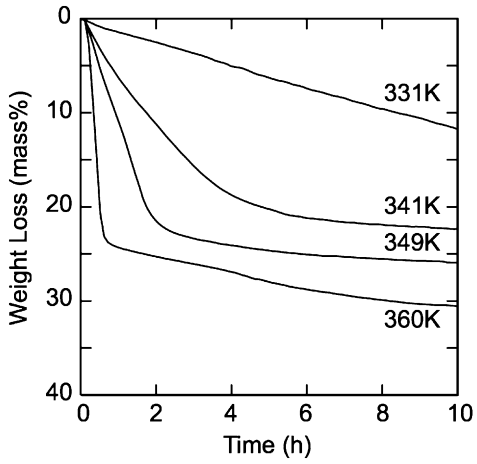

Fig. 4. Results of isothermal thermogravimetry at the temperatures of 331 K, 341 K, 349 K, and 360 K, under helium flow.

of $AlH_3 \cdot 0.19[(C_2H_5)_2O]$ is roughly estimated to be −54 kJ/mol. By a comparison with the formation enthalpy of γ-AlH_3 (-1.5 ± 0.8 kJ/mol [4]), it is suggested that γ-AlH_3 is largely stabilized by ether.

3.3. Desolvation and dehydriding reactions under isothermal process

Fig. 4 shows the isothermal TG profiles at 331 K, 341 K, 349 K, and 360 K. There are two different slopes corresponding to the rapid desolvation of ether and the slow desorption of hydrogen (which were also detected in the results of QM (not shown)). The initial rapid weight losses were caused by ether desolvation, which amounted to 22–25 mass% within 40 min, 2 h, and 6 h at 360 K, 349 K, and 341 K, respectively. These losses were smaller than the value of 31.5 mass% that was measured in the heating process (Fig. 2) because gradual desolvation and hydrogen desorption occurred during the time interval of each measurement.

Because the high temperature caused the desolvation reaction to proceed rapidly and since a short time is desirable for the preparation of AlH_3, the detailed decomposition process was directly observed by *in situ* XRD measurements at 349 K and 360 K in order to clarify the appropriate conditions. The results of the *in situ* XRD measurements at 349 K and 360 K are shown in Fig. 5(a) and (b), respectively, and their peak intensities are

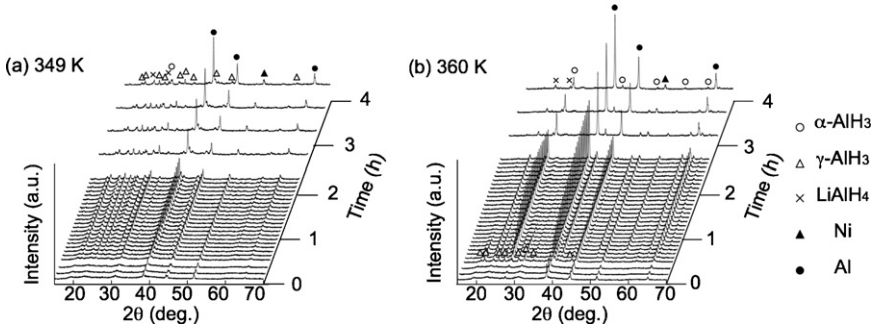

Fig. 5. Powder X-ray diffraction profiles (*in situ* measurements) at (a) 349 K and (b) 360 K. These measurements were carried out under vacuum.

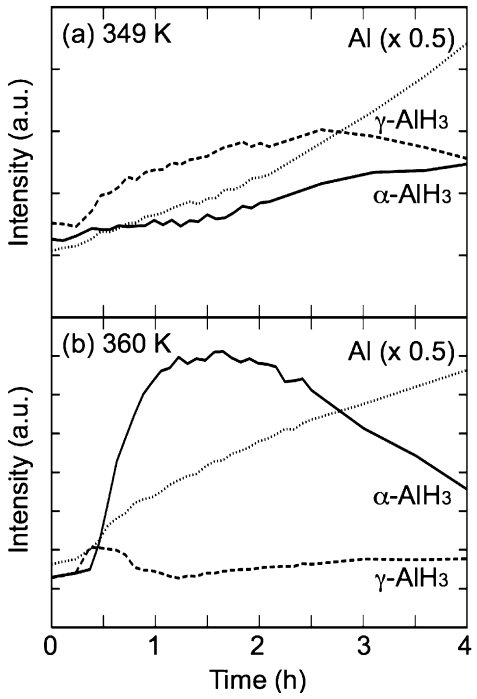

Fig. 6. Time dependences of the peak intensities of *in situ* powder X-ray diffraction profiles shown in figure. The 2θ of each peak is around 27.6°, 31.0°, and 38.5° for α-, γ-AlH_3, and metallic Al, respectively.

depicted in Fig. 6(a) and (b). At 349 K, γ-AlH_3 was the dominant phase until 1.5 h, and subsequently it started to transform into α-AlH_3. On the other hand, at 360 K, γ-AlH_3 appeared and immediately disappeared within a short time; α-AlH_3 then became the dominant phase after around 1 h. The intensities of the metallic Al increased at both the temperatures, probably indicating that the dehydriding reaction occurred continuously. The results can provide the appropriate conditions to effectively obtain α- and γ-AlH_3 by restraining the occurrence of the dehydriding reaction, for example, heating up to 349 K for 1.5 h and 360 K for 1 h in order to obtain γ- and α-AlH_3, respectively.

4. Conclusions

The thermal properties of AlH_3-etherate and its desolvation reaction into AlH_3 were experimentally investigated under heating and isothermal processes. γ-AlH_3-ehterate with the molecular formula $AlH_3 \cdot 0.19(C_2H_5)_2O$ was formed; no other etherates (such as α-AlH_3-etherate) were obtained in our studies. The steps in the decomposition reactions of γ-AlH_3-ehterate can be summarized as follows: (I) AlH_3-ehterate is desolvated to form γ-AlH_3 by an endothermic reaction starting at 350 K, (II) γ-AlH_3 immediately transforms into α-AlH_3 in an exothermic reaction above 373 K, and (III) the dehydriding reaction of α-AlH_3 proceeds along with an endothermic reaction for 405–440 K. The results of the isothermal measurements provided appropriate conditions to effectively obtain α- and γ-AlH_3 by restraining the occurrence of the dehydriding reaction.

Acknowledgements

The authors would like to thank Prof. H. Tobita and Dr. T. Komuro for valuable discussion. This work was financially supported by the Ministry of Education, Culture, Sports, Science and Technology, Japan, "Grant-in-Aid for Encouragement of Young Scientists (B) #17760555", and by the Office of Hydrogen, Fuel Cells, and Infrastructure Technologies of the US Department of Energy.

References

[1] G. Sandrock, J. Reilly, J. Graetz, W.-M. Zhou, J. Johnson, J. Wegrzyn, Appl. Phys. 80A (2005) 687–690.
[2] J. Graetz, J.J. Reilly, J. Phys. Chem. B 109 (2005) 22181.
[3] S. Orimo, Y. Nakamori, T. Kato, C. Brown, C.M. Jensen, Appl. Phys. A 80 (2006) 8–11.
[4] F.M. Brower, N.E. Matzek, P.F. Reigler, H.W. Rinn, C.B. Roberts, D.L. Schmidt, J.A. Snover, K. Terada, J. Am. Chem. Soc. 98 (1976) 2450–2453.
[5] P. Claudy, B. Bonnetot, J. Etienne, G. Turck, J. Therm. Anal. 8 (1975) 255–262.
[6] P. Claudy, B. Bonnetot, J.M. Letoffe, J. Therm. Anal. 15 (1979) 129–139.
[7] H. Wieser, W.G. Laidlaw, P.J. Krueger, H. Fuhrer, Spectrochim. Acta 24 (1968) 1055–1089.
[8] R.S. Chellappa, D. Chandra, S.A. Gramsch, R.J. Hemley, J.-F. Lin, Y. Song, J. Phys. Chem. B 110 (2006) 11088.
[9] C.-P. Wong, P.J. Miller, Energ. Mater. 23 (2005) 169–181.
[10] G. Pilcher, H.A. Skinner, A.S. Pell, A.E. Pope, Trans. Faraday Soc. 59 (1963) 316–330.